The Effect of Salt Stoichiometry on Protein–Salt Interactions Determined by Ternary Diffusion in Aqueous Solutions

Onofrio Annunziata,*,† Luigi Paduano,†,‡ and John G. Albright†

Department of Chemistry, Texas Christian University, Fort Worth, Texas 76129, and Dipartimento di Chimica, Università di Napoli "Federico II", Naples, 80126, Italy

We report the four diffusion coefficients for the lysozyme–MgCl$_2$–water ternary system at 25 °C and pH 4.5. The comparison with previous results for the lysozyme–NaCl–water ternary system is used to examine the effect of salt stoichiometry on the transport properties of lysozyme–salt aqueous mixtures. We find that the two cross-diffusion coefficients are very sensitive to salt stoichiometry. One of the cross-diffusion coefficients is examined in terms of common-ion, excluded-volume, and protein-preferential hydration effects. We use the four ternary diffusion coefficients to extract chemical-potential cross-derivatives and protein-preferential interaction coefficients. These thermodynamic data characterize the protein–salt thermodynamic interactions. We demonstrate the presence of the common-ion effect (Donnan effect) by analyzing the dependence of the preferential-interaction coefficient not only with respect to salt concentration but also with respect to salt stoichiometry. We conclude that the common-ion effect and the protein-preferential hydration are both important for describing the lysozyme–MgCl$_2$ thermodynamic interaction.

Introduction

The chemical potential of a protein component in aqueous solution is significantly affected by the presence of hydration, ligand binding, crowding, and Donnan effects.[1–12] One way to modify these factors is by varying the concentration of additives in solution. As a result, conformational changes,[2] protein precipitation, and protein crystallization may occur.[10–12] Understanding how the chemical potential of a protein is affected by the concentration of additives is important for (1) predicting conditions where phase transitions of protein solutions can occur and (2) understanding the mechanism of interaction between the protein and additives relevant to protein unfolding,[2,13] enzyme catalysis,[14] and ligand binding.[15]

Among all additives, salts are clearly the most employed in protein solutions. In small amounts (<0.1 M), salts are used as buffer components and to reproduce physiological conditions. In larger amounts, they find important applications in protein crystallization, protein purification by precipitation,[10] protein unfolding (e.g., guanidinium hydrochloride),[16] and salt-induced activation of lyophilized enzymes in organic solvents.[14]

The effect of salt on the thermodynamics of protein solutions has been extensively studied, especially in relation to lysozyme–NaCl aqueous systems. The second virial coefficient, B_2, determined by light[17] and X-ray scattering,[18] has been the primary parameter for investigating the action of salts on proteins. This parameter characterizes protein–protein net interactions in solutions. Although B_2 is very important in addressing the effect of salt type and concentration on protein–protein interactions, it does not directly probe protein–salt interactions. This is an essential ingredient for explaining the effect of salt on the thermodynamics of protein solutions,

especially at the high salt concentrations relevant to protein crystallization, precipitation, unfolding, and enzyme catalysis. To obtain a more complete description of the action of salt ions on proteins, experimental techniques that can directly probe protein–salt interactions must be employed. Equilibrium dialysis[1] and vapor pressure osmosis[3] has been used for determining the effect of salt concentration on the protein chemical potential, i.e., the first derivative of the protein chemical potential with respect to the salt concentration. Most of these results have been interpreted in terms of protein preferential hydration and/or binding of salt ions.

The dependence of the chemical potential of a macromolecule on salt concentration is also central for understanding diffusive mass transport of proteins. One consequence of this thermodynamic aspect is that a gradient of salt concentration can generate a gradient of protein chemical potential and vice versa.[19] This implies that the diffusion of salt and protein are coupled. In the case of a ternary protein–saltwater solution, protein–salt coupled diffusion is described by a matrix of four diffusion coefficients.[19–21] Clearly, this diffusion matrix can be used to probe protein–salt interactions.

Recently, we have introduced a novel method based on ternary diffusion measurements for determining the effect of salt concentration on the protein chemical potential.[9,19] We applied this method to lysozyme in the presence of three 1:1 electrolyte cases: NaCl,[9] KCl,[19] and NH$_4$Cl.[22] The precision of these extracted data allowed us to extract the first derivative of the protein chemical potential as a function of salt concentration. Using our results, we have determined two mechanisms of action of salts on lysozyme–salt interactions. The main mechanism of action is not preferential hydration but the common-ion effect,[9] also known as the Donnan effect,[23] which is commonly believed to become negligible for salt concentrations higher than 0.1 M.[24] We have found that the common-ion effect is significant at salt concentrations relevant to protein crystallization and precipitation (0.2–1.5 M). Furthermore, the

* To whom correspondence should be addressed. E-mail: O.Annunziata@tcu.edu. Telephone: (817) 257-6215. Fax: (817) 257-5851.
† Texas Christian University.
‡ Università di Napoli "Federico II".

common-ion effect is essential for explaining the diffusion properties of lysozyme−salt solutions.[9]

We remark that the common-ion effect is intimately related to the salt stoichiometry. For this reason, it is very valuable to analyze the effect of 2:1 electrolytes on the thermodynamic and diffusion properties of lysozyme solutions. In this paper, we present the first study of lysozyme−salt coupled diffusion in the presence of a 2:1 electrolyte. We report ternary diffusion measurements on the lysozyme−MgCl$_2$−water system at 25 °C and pH 4.5. Experiments were performed at 0.6 mM (≈ 8.6 mg/mL) lysozyme and 0.09−2.00 M MgCl$_2$ concentrations. Our experimental results are compared here with those previously obtained for the lysozyme−NaCl−water system.[19,21] The central objective of this paper is to describe diffusion and thermodynamics of proteins in the presence of 2:1 electrolyte solutions by applying common-ion, excluded-volume, and preferential-hydration concepts.

Ternary Diffusion Coefficients

For the protein(1)−salt(2)−water(0)[25] ternary system, multicomponent diffusion is described by the extended Fick's first law:[20,21,26]

$$-J_1 = D_{11}\nabla C_1 + D_{12}\nabla C_2 \quad (1a)$$

$$-J_2 = D_{21}\nabla C_1 + D_{22}\nabla C_2 \quad (1b)$$

Here, C_1 and C_2 are molar concentrations of the two solutes, J_1 and J_2 are the corresponding fluxes, and the four D_{ij}'s (with $i,j = 1,2$) are the diffusion coefficients. Main-diffusion coefficients, D_{11} and D_{22}, describe the flux of a solute due to its own concentration gradient, while cross-diffusion coefficients, D_{12} and D_{21}, describe the flux of a solute due to the concentration gradient of the other solute.

Diffusion can be described relative to different reference frames.[27] Thus eq 1a,b is applicable in volume-fixed (subscript V), solvent-fixed (subscript 0), and other frames. Diffusion coefficients are measured in the laboratory-fixed frame, which is an excellent approximation of the $(D_{ij})_V$ values in the volume-fixed frame. The $(D_{ij})_0$ values can be easily calculated from the $(D_{ij})_V$ values and the partial molar volumes, $\bar{V}_i$, obtained from density measurements.[28−30]

From irreversible thermodynamics, the fundamental driving forces for diffusion are the chemical potential gradients of the mixture components. Thus, isothermal ternary diffusion can be described in terms of the Onsager diffusion coefficients (ODCs) L_{ij} and the chemical potential gradients $\nabla\mu_i$. The corresponding linear laws are:

$$-J_1 = L_{11}\nabla\mu_1 + L_{12}\nabla\mu_2 \quad (2a)$$

$$-J_2 = L_{21}\nabla\mu_1 + L_{22}\nabla\mu_2 \quad (2b)$$

In the solvent frame, the Onsager reciprocal relation (ORR)[28−31] is:

$$(L_{12})_0 = (L_{21})_0 \quad (3)$$

We can use eqs 1a,b and 2a,b in the solvent frame to relate the diffusion coefficients, $(D_{ij})_0$, to the ODCs, $(L_{ij})_0$, and the chemical potential derivatives, $\mu_{ij} \equiv (\{\partial\mu_i\}/\{\partial C_j\})_{T,p,C_k,k\neq j}$, where T is the temperature and p the pressure:

$$(D_{11})_0 = (L_{11})_0\,\mu_{11} + (L_{12})_0\,\mu_{21} \quad (4a)$$

$$(D_{12})_0 = (L_{11})_0\,\mu_{12} + (L_{12})_0\,\mu_{22} \quad (4b)$$

$$(D_{21})_0 = (L_{21})_0\,\mu_{11} + (L_{22})_0\,\mu_{21} \quad (4c)$$

$$(D_{22})_0 = (L_{21})_0\,\mu_{12} + (L_{22})_0\,\mu_{22} \quad (4d)$$

Using eq 3 and the equality of the molality-based chemical-potential cross-derivatives, eq 4a−d can be solved with respect to μ_{12} and μ_{21}, yielding:[19]

$$\mu_{12} = [\mu_{11}[C_1\bar{V}_2(D_{22})_0 - (1 - C_1\bar{V}_1)(D_{12})_0] - \mu_{22}[C_2\bar{V}_1(D_{22})_0 - (1 - C_1\bar{V}_1)(D_{21})_0]]/ [(1 - C_2\bar{V}_2)(D_{22})_0 - (1 - C_1\bar{V}_1)(D_{11})_0] \quad (5a)$$

$$\mu_{21} = [\mu_{11}[C_1\bar{V}_2(D_{11})_0 - (1 - C_2\bar{V}_2)(D_{12})_0] - \mu_{22}[C_2\bar{V}_1(D_{11})_0 - (1 - C_2\bar{V}_2)(D_{21})_0]]/ [(1 - C_2\bar{V}_2)(D_{22})_0 - (1 - C_1\bar{V}_1)(D_{11})_0] \quad (5b)$$

where the partial molar volumes, $\bar{V}_i$, are expressed in dm^3 mol^{-1}.

We can express the chemical potential derivatives in terms of molar concentrations and mean ionic activity coefficients, y_i. If the stoichiometric coefficients for the cations (i.e., lysozyme and magnesium) is taken to be unity, we obtain the following relationships:[31]

$$\frac{\mu_{11}}{RT} = \frac{1}{C_1} + \frac{z_p{}^2}{z_pC_1 + z_MC_2} + (z_p + 1)\frac{\partial\ln y_1}{\partial C_1} \quad (6a)$$

$$\frac{\mu_{12}}{RT} = \frac{z_Mz_p}{z_pC_1 + z_MC_2} + (z_p + 1)\frac{\partial\ln y_1}{\partial C_2} \quad (6b)$$

$$\frac{\mu_{21}}{RT} = \frac{z_Mz_p}{z_pC_1 + z_MC_2} + (1 + z_M)\frac{\partial\ln y_2}{\partial C_1} \quad (6c)$$

$$\frac{\mu_{22}}{RT} = \frac{1}{C_2} + \frac{z_M{}^2}{z_pC_1 + z_MC_2} + (1 + z_M)\frac{\partial\ln y_2}{\partial C_2} \quad (6d)$$

where z_p and z_M are, respectively, the charge of the protein and the charge of the salt cation.

Parts a and b of eq 5 can be used to calculate μ_{12} and μ_{21} from the $(D_{ij})_0$'s and $\bar{V}_i$'s and estimates of μ_{11} and μ_{22}.[19] The value of μ_{11} is obtained by neglecting the nonideal term $(z_p + 1)(\partial\ln y_1/\partial C_1)$ in eq 6a. The value of z_p can be initially set equal to that extracted by titration experiments. We will show in Results that we can obtain a more appropriate value of z_p from our μ_{12} and μ_{21} results. We remark that our calculated values of μ_{12} and μ_{21} are rather insensitive to the accuracy of μ_{11} estimates; indeed, we find that a 5-fold change in μ_{11} values lead to an error of less than 5% in both μ_{12} and μ_{21}. According to second-virial-coefficient estimates, the nonideal term is about 10% of the ideal term in μ_{11}.[9] We thus conclude that more accurate estimates of μ_{11} are not necessary. The value of μ_{22} is obtained by taking $(z_M + 1)(\partial\ln y_2/\partial C_2)$ from the activity-coefficient data available on the binary salt-water systems. These estimates of μ_{22} can be considered accurate because the protein concentration is low. Indeed, the ternary salt main-diffusion coefficient, $(D_{22})_0$, is only 1−2% lower than the corresponding binary value within our experimental concentration ranges. Moreover, this small difference is nearly independent of salt concentration. Thus we can relate it to the obstruction effect of proteins on salt diffusion rather than to changes in μ_{22}.[9,19]

Salt Stoichiometry on Protein—Salt Interactions

J. Phys. Chem. B, Vol. 110, No. 32, 2006 **16141**

TABLE 1: Ternary Diffusion Coefficients for the Lysozyme—MgCl$_2$—H$_2$O System at 25 °C and pH 4.5

$\bar{\bar{C}}_1$ (mM)	0.5997	0.5992	0.5975	0.5987	0.5996	0.5996
$\bar{\bar{C}}_2$ (M)	0.0931	0.2326	0.4642	0.9304	1.5994	1.9995
$\bar{V}_0$ (cm^3 mol^{-1})	18.076	18.058	18.050	18.015	17.930	17.874
$\bar{V}_1$ (cm^3 mol^{-1})	10190	10240	10080	10230	10180	10200
$\bar{V}_2$ (cm^3 mol^{-1})	17.36	19.31	20.89	23.11	26.63	28.08
$(D_{11})_V$ (10^{-9} m^2 s^{-1})	0.1270 ± 0.0002	0.1145 ± 0.0001	0.1019 ± 0.002	0.0833 ± 0.0002	0.0640 ± 0.0001	0.0548 ± 0.0002
$(D_{12})_V$ (10^{-12} m^2 s^{-1})	0.799 ± 0.008	0.324 ± 0.003	0.201 ± 0.007	0.145 ± 0.006	0.156 ± 0.004	0.151 ± 0.005
$(D_{21})_V$ (10^{-9} m^2 s^{-1})	3.5 ± 0.2	4.4 ± 0.1	6.8 ± 0.2	12.3 ± 0.2	21.4 ± 0.1	26.0 ± 0.2
$(D_{22})_V$ (10^{-9} m^2 s^{-1})	1.034 ± 0.001	1.025 ± 0.001	1.040 ± 0.002	1.080 ± 0.002	1.113 ± 0.001	1.102 ± 0.001
$(D_{11})_0$ (10^{-9} m^2 s^{-1})	0.1278	0.1153	0.1026	0.0804	0.0648	0.0556
$(D_{12})_0$ (10^{-12} m^2 s^{-1})	0.815	0.338	0.215	0.170	0.176	0.172
$(D_{21})_0$ (10^{-9} m^2 s^{-1})	3.6	4.7	7.4	13.4	23.5	28.7
$(D_{22})_0$ (10^{-9} m^2 s^{-1})	1.036	1.030	1.051	1.105	1.166	1.171

TABLE 2: Chemical Potential Derivatives and ODCs for the Lysozyme—MgCl$_2$—H$_2$O System

C_2 (M)	μ_{11}/RT (M^{-1})	μ_{22}/RT (M^{-1})	μ_{12}/RT (M^{-1})	μ_{21}/RT (M^{-1})	$RT(L_{11})_0/C_1$ (10^{-9} m^2 s^{-1})	$RT(L_{12})_0/C_1$ (10^{-9} m^2 s^{-1})	$RT(L_{22})_0/C_2$ (10^{-9} m^2 s^{-1})
0.093	2003	27.303	77.1	103.5	0.220	−0.29	0.413
0.233	1805	11.924	28.3	56.9	0.144	−0.22	0.373
0.464	1742	6.938	17.3	49.8	0.105	−0.21	0.327
0.930	1705	4.714	12.9	57.8	0.088	−0.18	0.252
1.599	1688	4.111	16.7	83.4	0.076	−0.24	0.178
2.000	1684	4.076	17.9	100.6	0.069	−0.23	0.144

The largest source of error in μ_{12} and μ_{21} comes from the uncertainty of the $(D_{21})_0$ values. The uncertainty of μ_{21} is at least three times lower than that of μ_{12}. A conservative estimation of the error of $(D_{21})_0$ is ±0.2 × 10^{-9} m^2 s^{-1} for all cases (see Table 1). On this basis, the uncertainty of μ_{12} in the lysozyme—MgCl$_2$ experiments is ≈9% at C_2 = 0.09 M and drops to ≈4% at C_2 > 1.0 M. We note that the uncertainty of μ_{12} in the 1:1 electrolyte systems was 2−3%.

Materials and Methods

Materials. Six-times recrystallized and lyophilized egg-white lysozyme (HEWL) was purchased from Seikagaku America and used without further purification.[21] A protein—water stock solution was prepared by weight using double-distilled water. The molecular weight of HEWL was taken to be 14 307 g mol^{-1}. Corrections were made for the chloride ion weight fraction in the HEWL samples as shown in ref 21. Mallinckrodt AR MgCl$_2$·6H$_2$O was used without further purification. A MgCl$_2$—water stock solution was prepared and its density was carefully measured at 25 °C. This density value was used to calculate MgCl$_2$ concentration from the available density—concentration relation.[31]

Methods. The Gosting diffusiometer and its modifications, density measurements, solution preparation, pH adjustment, and data reduction procedures are described in our previous papers.[19,21] In brief, solutions for diffusion measurements were prepared by adding known weights of lysozyme and MgCl$_2$ stock solutions. Water was then used to dilute the solution almost to the final volume. The pH of the solution was then adjusted to 4.5 by using a few drops of a HCl—water stock solution (pH 1.2). A Corning 135 pH meter with an Orion 8102 ROSS combination pH electrode, standardized with Corning reference solutions, was used to measure the pH. The final volume was then reached by adding water, and the pH remeasured to confirm its value of 4.5.

Ternary mutual diffusion coefficients were measured at 25.00 °C with the Gosting diffusiometer operating in the Rayleigh interferometric optical mode. The instrument has been upgraded with a laser light source and a vertical linear 6 cm 6000 pixel photodiode scanning array at the image position. A stepping motor moved the array horizontally across the Rayleigh inter-

ferometric pattern and data were recorded at 10 μ horizontal intervals. This gives the two-dimensional light-intensity distribution of the Rayleigh pattern, which yields the refractive-index profile inside the diffusion cell. We obtained 50 refractive-index profiles during the course of each experiment. Experiments were performed by the free-diffusion method in a 10 cm vertical diffusion cell with a 2.5 cm horizontal optical path length and a 0.3 cm width. The temperature was regulated to ±0.001 °C precision and ±0.01 °C accuracy. Initial step-function distributions of solute concentrations were prepared with the boundary located at the center of the cell. All experimental data were obtained before detectable concentration changes occurred at the top and bottom ends of the cell, consistent with the free-diffusion boundary condition. A minimum of two experiments are required for determining the four diffusion coefficients at a given set of mean concentrations ($\bar{\bar{C}}_1$, $\bar{\bar{C}}_2$ in Table 1). These two experiments must have different combinations of solute concentration differences across the diffusion boundary. To verify reproducibility, two other duplicate experiments were performed at each set of mean concentrations. More experimental details are available in the Supporting Information.

Results

In Table 1, we report the volume-fixed $(D_{ij})_V$ values calculated with data from all four experiments at each of the six MgCl$_2$ concentrations. Table 1 also includes the partial molar volumes $\bar{V}_0$, $\bar{V}_1$, $\bar{V}_2$ obtained from density measurements. Solvent frame $(D_{ij})_0$ are calculated from the $(D_{ij})_V$ and $\bar{V}_i$ by using eq 2 in ref 28. Tables with detailed results for each diffusion experiment are available in the Supporting Information.

In Table 2, we report the values of μ_{11}/RT and μ_{22}/RT, obtained using the procedures described in the previous section, and the values of μ_{12}/RT and μ_{21}/RT, obtained from eq 5a,b. Table 2 also includes $RT(L_{ij})_0$ values calculated from eq 4a−d (explicit relations are given by eq 7 in ref 19).

In Figure 1a−d, we show the four diffusion coefficients as functions of C_2 at C_1 = 0.6 mM for the MgCl$_2$ case. For comparison, we include the previously reported $(D_{ij})_V$ values for the NaCl case[21] (at pH 4.5). In Figure 1d, we include binary saltwater data[32,33] (dashed curves) together with the $(D_{22})_V$ ternary results.
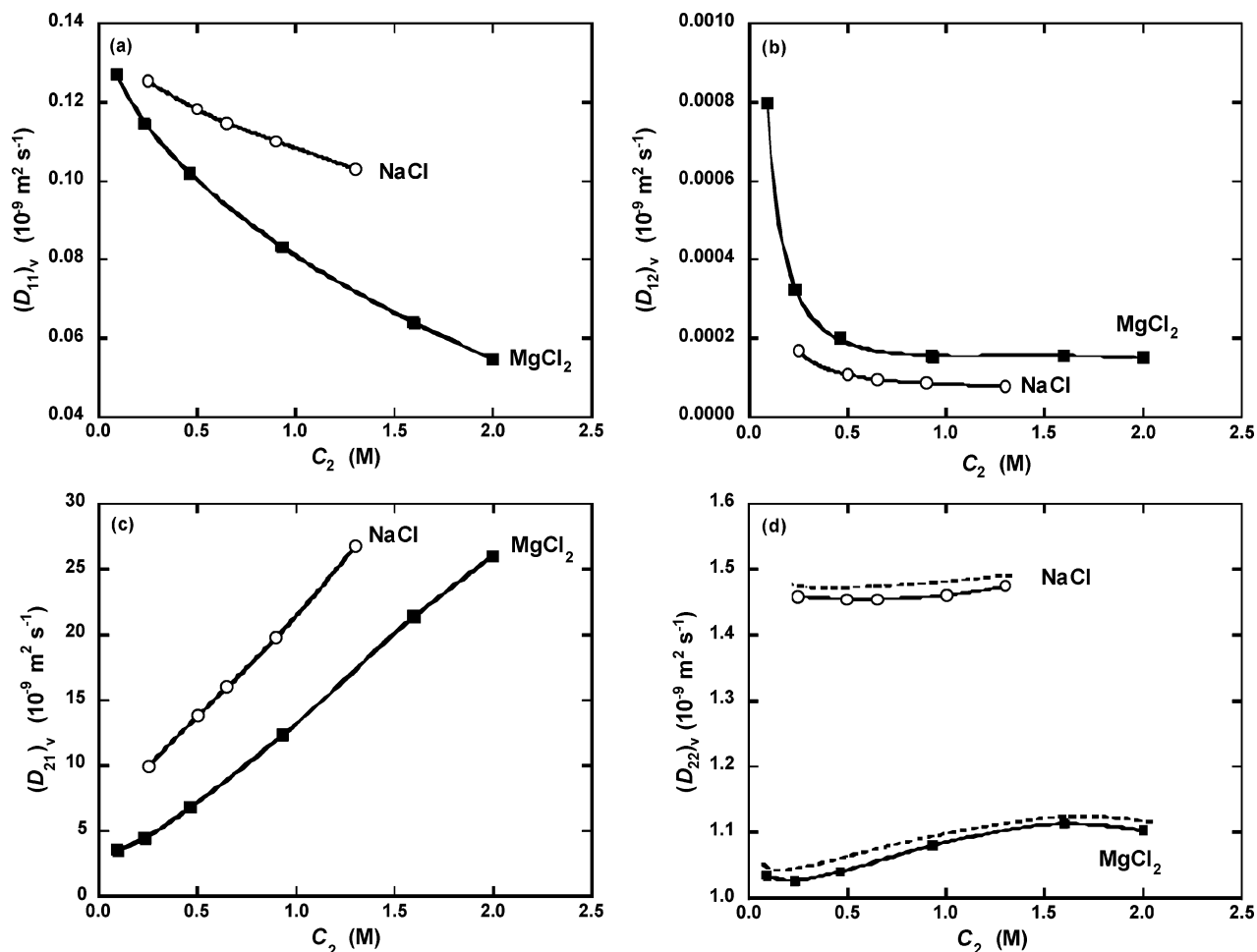
Figure 1. Volume-fixed diffusion coefficients as functions of salt concentration, C_2, for the lysozyme$-$NaCl$-$H$_2$O ($\bigcirc$) and the lysozyme$-$MgCl$_2-$H$_2$O ($\blacksquare$) systems at $C_1 = 0.6$ mM, pH 4.5, and 25 °C: (a) $(D_{11})_V$, (b) $(D_{12})_V$, (c) $(D_{21})_V$, (d) $(D_{22})_V$. The solid curves are smoothed through the ternary experimental points. The dashed curves are smoothed through the omitted binary diffusion coefficients for the salt components; data taken from ref 33 (NaCl) and ref 32 from the (MgCl$_2$).
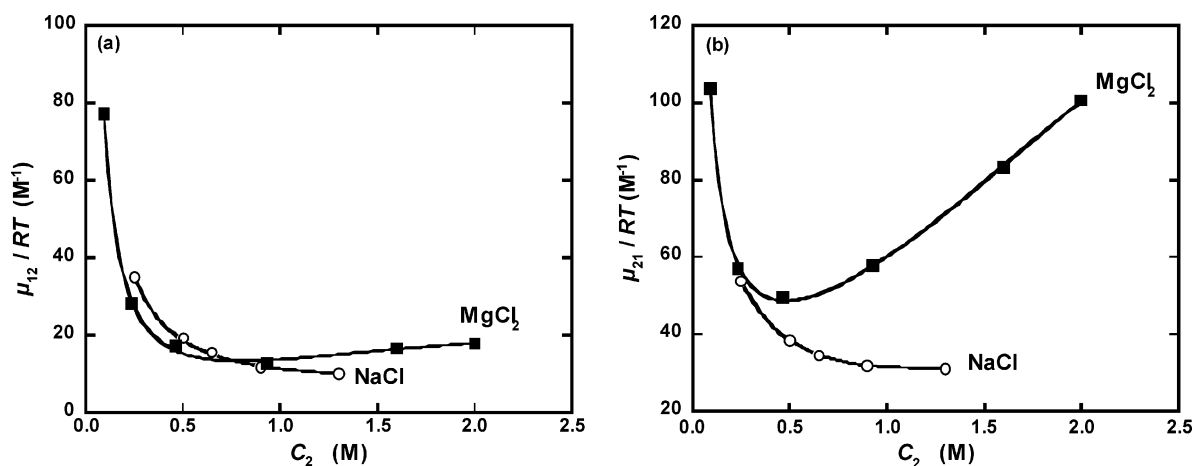
Figure 2. Chemical-potential cross-derivatives as a function of salt concentration, C_2, for the lysozyme$-$NaCl$-$H$_2$O ($\bigcirc$) and the lysozyme$-$MgCl$_2-$H$_2$O ($\blacksquare$) systems. The solid curves are fits to the data using eq 6b for $\mu_{12}/(RT)$ and eq 6c for $\mu_{21}/(RT)$, where the activity-coefficient derivatives are expressed as polynomial functions of C_2.

In Figure 2a,b, we report μ_{12}/RT and μ_{21}/RT for the MgCl$_2$ case as a function of salt concentration. In the same figure, we include our results for the NaCl case.[19] At low salt concentrations, the values of μ_{12}/RT and μ_{21}/RT sharply decrease. This is consistent with eq 6b,c, in which $z_p z_M/(z_p C_1 + z_M C_2)$ is a dominant term that varies approximately as z_p/C_2. By expanding both activity coefficient derivatives as polynomial functions in

$(z_p C_1 + z_M C_2)$ and applying nonlinear regression to eq 6b,c, we calculate experimental value of $z_p = 8 \pm 1$ for lysozyme in the aqueous lysozyme$-$MgCl$_2$ mixtures. This is in agreement with the value of $z_p = 9 \pm 1$ we have previously obtained for NaCl.[19] The values of z_p obtained by fitting μ_{12}/RT and μ_{21}/RT correspond to the protein cation's effective charges, and they are lower than the experimental titration charges due to

Salt Stoichiometry on Protein−Salt Interactions

J. Phys. Chem. B, Vol. 110, No. 32, 2006 **16143**

counterion binding. Because the titration charge is ~11,[34] we estimate that ~3 chloride ions effectively move with one lysozyme molecule.

At high MgCl$_2$ concentrations, both μ_{12}/RT and μ_{21}/RT increases with C_2. This behavior is not observed in the case of NaCl. As we shall see later, the increase in μ_{12} and μ_{21} observed for MgCl$_2$ is related to the strong nonideality behavior of the binary MgCl$_2$−water system compared to the binary NaCl−water system.

Discussion

In this section, we will first review two important diffusion models used as references for interpreting our results. We will then examine the behavior of the four diffusion coefficients for the lysozyme−MgCl$_2$−water system and compare our results with those previously obtained for the lysozyme−NaCl−water system. This will allow us to determine the effect of salt stoichiometry on the diffusion coefficients. Finally, we will discuss our findings on the protein−salt thermodynamic interactions. One important feature of our systems is that the molar concentration of lysozyme is significantly lower than the salt concentration, i.e., $z_pC_1 \ll z_MC_2$. This condition will be used throughout our discussion.

Diffusion of charged macromolecules in the presence of an electrolyte solution can be discussed in terms of two important models: (a) the Nernst−Hartley equations,[26] which apply to an ideal-dilute ternary solution with two ionic components, and (b) the Stokes−Einstein equation,[23] which describes the tracer diffusion coefficient (or mobility) of macromolecules in the limit of $C_1 \rightarrow 0$. For both models, the diffusion coefficients are independent of frame because they apply at infinite dilution.

Nernst−Hartley Equations. At infinite dilution, the four diffusion coefficients of two ionic components with a common ion are related to the ionic mobilities of the three constituent ionic species. Because of electrostatic coupling (i.e., electroneutrality), the three ionic species cannot move independently. This coupled transport is described by the Nernst−Hartley (N−H) equations.

For our ternary electrolyte system, the N−H equations are:

$$D_{11} = \tilde{D}_p\left[1 + \frac{z_p{}^2C_1}{\Delta}(\tilde{D}_{Cl} - \tilde{D}_p)\right] \tag{7a}$$

$$D_{12} = \tilde{D}_p\frac{z_pz_MC_1}{\Delta}(\tilde{D}_{Cl} - \tilde{D}_M) \tag{7b}$$

$$D_{21} = \tilde{D}_M\frac{z_pz_MC_2}{\Delta}(\tilde{D}_{Cl} - \tilde{D}_p) \tag{7c}$$

$$D_{22} = \tilde{D}_M\left[1 + \frac{z_M{}^2C_2}{\Delta}(\tilde{D}_{Cl} - \tilde{D}_M)\right] \tag{7d}$$

where $\Delta = z_pC_1(z_p\tilde{D}_p + \tilde{D}_{Cl}) + z_MC_2(z_M\tilde{D}_M + \tilde{D}_{Cl})$. In eq 7a−d, $\tilde{D}_p$, $\tilde{D}_M$, and $\tilde{D}_{Cl}$ are, respectively, the tracer diffusion coefficients of the protein cation, salt co-ion (Na$^+$, $z_M = 1$; Mg^{2+}, $z_M = 2$), and chloride ion (common ion). The value of $\tilde{D}_p = 0.132 \times 10^{-9}$ m^2 s^{-1} for lysozyme (in aqueous NaCl at pH 4.5) was taken from ref 34. The tracer diffusion coefficients for small ions have been calculated from limiting ionic mobilities. For Na$^+$, Mg^{2+}, and Cl$^-$, they are 1.33, 0.706, and 2.03×10^{-9} m^2 s^{-1}, respectively.[35,36]

We are interested in the case where $z_pC_1 \ll z_MC_2$. Because $\tilde{D}_p < \tilde{D}_M$, $\tilde{D}_{Cl}$, we can write $\Delta = z_MC_2(z_M\tilde{D}_M + \tilde{D}_{Cl})$. Thus, eq 7a−d, which now apply under the conditions of $C_2 \rightarrow 0$ and $z_pC_1 \ll z_MC_2$, become:

$$D_{11} = \tilde{D}_p\left(1 + \frac{z_p{}^2C_1}{z_MC_2}\frac{\tilde{D}_{Cl} - \tilde{D}_p}{z_M\tilde{D}_M + \tilde{D}_{Cl}}\right) \tag{8a}$$

$$D_{12} = \tilde{D}_p\frac{z_pC_1}{C_2}\frac{\tilde{D}_{Cl} - \tilde{D}_M}{z_M\tilde{D}_M + \tilde{D}_{Cl}} \tag{8b}$$

$$D_{21} = z_p\frac{\tilde{D}_M(\tilde{D}_{Cl} - \tilde{D}_p)}{z_M\tilde{D}_M + \tilde{D}_{Cl}} \tag{8c}$$

$$D_{22} = (z_M + 1)\frac{\tilde{D}_M\tilde{D}_{Cl}}{z_M\tilde{D}_M + \tilde{D}_{Cl}} \tag{8d}$$

Compared to eq 7a−d, eq 8a−d has the advantage of showing the dominant forms of dependence of the four diffusion coefficients on the salt concentration and stoichiometry (i.e., z_M).

Although the N−H equations are only exact in the limits of both C_1 and C_2 approaching zero, they still provide an important reference tool for interpreting our experimental results. Because of their dependence on salt stoichiometry, the N−H equations are especially valuable when we will discuss the effect of salt type on the two cross-diffusion coefficients.

Stokes−Einstein Equation. At infinite dilution, the protein tracer diffusion coefficient, $\tilde{D}_p$, is often interpreted using the Stokes−Einstein equation: $\tilde{D}_p = k_BT/(6\pi r_H^{eq}\eta)$, where k_B is Boltzmann's constant, r_H^{eq} is the equivalent hydrodynamic radius, and η is the viscosity of the surrounding fluid, i.e., the interstitial saltwater medium.[23] As the salt concentration increases, viscosity increases for both the NaCl and MgCl$_2$ cases, and $\tilde{D}_p$ decreases. Because D_{11} and D_{12} are directly proportional to $\tilde{D}_p$ according to eq 8a,b, we will use the Stokes−Einstein equation to assess the role of viscosity on the observed dependence of these two diffusion coefficients on salt type and concentration.

We will now examine each ternary diffusion coefficient. Because our thermodynamic results were obtained from the solvent-frame diffusion coefficients, we will address in particular the behavior of the $(D_{ij})_0$'s. Yet the difference between the values of $(D_{ij})_V$ and $(D_{ij})_0$ is small and irrelevant for the interpretations reported below.

Examination of D_{11}. Values of $(D_{11})_V$ for the lysozyme−MgCl$_2$ and lysozyme−NaCl systems are shown in Figure 1a. In the MgCl$_2$ case, the diffusion coefficient D_{11} (i.e., $(D_{11})_V$ and $(D_{11})_0$) significantly decreases as the salt concentration increases. At $C_2 = 2.0$ M, D_{11} reduces to ≈50% of its value at 0.09 M. In the case of NaCl, this decrease is significantly smaller.

The observed behavior of D_{11} for both salts can be ascribed to at least two factors. According to the Stokes−Einstein equation and eq 8a, we expect the D_{11} values to decrease as solution viscosity increases. To examine this effect, we consider the product $(D_{11})_0(\eta/\eta_0)$, where η is the viscosity of the corresponding binary saltwater systems[37,38] and η_0 is the viscosity of water. In Figure 3, we plot $(D_{11})_0(\eta/\eta_0)$ as a function of C_2. Clearly, this viscosity correction removes much of the D_{11} dependence on salt type and concentration. We have previously shown that this applies to the KCl and NH$_4$Cl cases as well.[9]

From Figure 3, we can see that, at low salt concentration, $(D_{11})_0(\eta/\eta_0)$ decreases as C_2 increases for both salts. This result can be explained by analyzing eq 8a, which shows that D_{11} decreases as C_2 increases. This behavior is related to the electrostatic dragging effect of the faster chloride ions exerted on the positively charged proteins. Indeed, we have previously
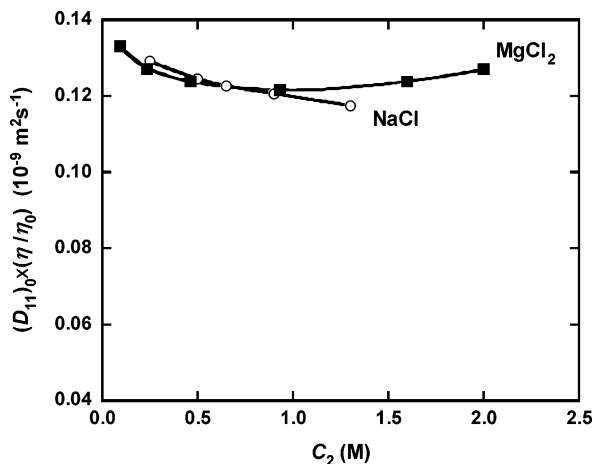
Figure 3. Viscosity-corrected $(D_{11})_0(\eta/\eta_0)$ as a function of salt concentration, C_2, for the lysozyme−NaCl−H_2O (○) and the lysozyme−$MgCl_2$−H_2O (■) systems. The solid curves are smoothed through the ternary experimental points.

Figure 4. Corrected cross-diffusion coefficient $(D_{12})_0(\eta/\eta_0)/W_0$ as a function of salt concentration, C_2, for the lysozyme−NaCl−H_2O (○) and the lysozyme−$MgCl_2$−H_2O (■) systems. The solid curves are smoothed through the ternary experimental points.

reported that the diffusion coefficient of the lysozyme chloride component in pure water (0.54×10^{-9} m^2 s^{-1} at pH 4.5) is about four times higher than the lysozyme tracer diffusion coefficient.[19,21] As the salt concentration increases, this dragging effect diminishes due to the presence of co-ion electrostatic shielding.

To emphasize the dependence of D_{11} on concentration, we rewrite eq 8a as $D_{11} = \tilde{D}_P (1 + \alpha(C_1/C_2))$. If we use the above-reported tracer diffusion coefficients, we estimate $\alpha = 46$ for the $MgCl_2$ case and $\alpha = 18$ for the NaCl case, thereby implying that, at a given salt concentration, D_{11} for the $MgCl_2$ case is higher than D_{11} for the NaCl case. This is indeed what we observe at low salt concentration ($C_2 \leq 0.5$ M in Figure 3). At high salt concentration, the interpretation of the specific behavior of $(D_{11})_0(\eta/\eta_0)$ becomes more difficult and needs to take into account protein conformational changes and specific effects of salt ions on protein−protein interactions. Assuming that hydrodynamic-radius changes can be ignored, our results at high salt concentrations suggest an increase of μ_{11} and a corresponding increase of protein−protein repulsive interactions. The presence of protein−protein repulsive interactions for lysozyme at high $MgCl_2$ concentrations has previously been argued by Grygsby et al.[39] using dynamic light scattering.

Examination of D_{22}. Values of $(D_{22})_V$ for the lysozyme−$MgCl_2$ and lysozyme−NaCl systems are shown in Figure 1d. The ternary D_{22} values are just 1−2% lower than the corresponding binary values. As mentioned earlier, this implies that our estimates of μ_{22} from binary activity coefficients are highly accurate. The small difference between the ternary and binary values is consistent with an expected small obstruction effect of the protein macromolecules on the motion of the small salt ions.

Examination of D_{12}. Values of $(D_{12})_V$ for the lysozyme−$MgCl_2$ and lysozyme−NaCl systems are shown in Figure 1b. This cross-diffusion coefficient describes how the flux of lysozyme is affected by the salt concentration gradient. From Figure 1b, we can see that, at the low concentrations, D_{12} decreases significantly as C_2 increases for both salts. This behavior can be qualitatively understood from the N−H equations. In the presence of a gradient of salt concentration, a flux of both chloride and metal ions is generated. Because $\tilde{D}_{Cl} > \tilde{D}_M$, the chloride ions will electrostatically drag both the positively charged proteins and the metal ions depending on their relative amounts: C_1/C_2. This is the reason D_{12} is inversely
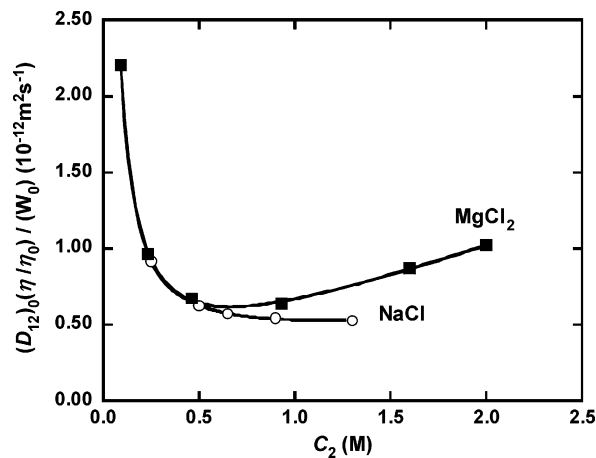
proportional to C_2 and directly proportional to $\tilde{D}_{Cl} - \tilde{D}_M$. From the values of the tracer diffusion coefficients listed above, it is expected that D_{12} will be larger for $MgCl_2$ than for NaCl at a given salt concentration. This is consistent with our experimental results (see Figure 1b). Nevertheless, we observe that the N−H equations poorly predict the experimental values of D_{12} even at low salt concentration.

From Table 2, we also note that $(L_{11})_0\mu_{12} \approx -(L_{12})_0\mu_{22}$,[9] which implies that D_{12} is a small difference between two larger contributions (see eq 4b). This indicates that the prediction of D_{12} from estimates of the Onsager diffusion coefficients is also difficult. Nonetheless, we can still attempt to understand the effect of salt type on D_{12} by rearranging eq 4b in the form of the following product:[9]

$$(D_{12})_0 = (L_{11})_0\mu_{12}W \tag{9}$$

where

$$W = 1 + \frac{(L_{12})_0}{(L_{11})_0}\frac{\mu_{22}}{\mu_{12}} \tag{10}$$

In the limit, where $C_2 \rightarrow 0$ and $C_1/C_2 \rightarrow 0$, we can use eq 28 of ref 40 with the limiting values to obtain

$$W_0 = \frac{\tilde{D}_{Cl} - \tilde{D}_M}{z_M\tilde{D}_M + \tilde{D}_{Cl}} \tag{11}$$

The mobility ratio, W_0, and the viscosity correction, (η/η_0), are the only two properties that directly depend on the type of saltwater binary system. We remove these factors by computing a corrected diffusion coefficient, $(D_{12})_0(\eta/\eta_0)/W_0$, for both salt cases. According to N−H equations and Stokes−Einstein equation, $(D_{12})_0 (\eta/\eta_0)/W_0$ should not depend on salt type. From Figure 4, we can see that there is virtually no detectable difference between the two salt cases at $C_2 < 0.5$ M. At high salt concentration, we find that $(D_{12})_0(\eta/\eta_0)/W_0$ for the $MgCl_2$ case increases with C_2 contrary to what we observe for NaCl. Although the observed difference is of difficult interpretation, we note that, according to eq 9, $(D_{12})_0$ is proportional to μ_{12}. We indeed observe that the difference in the behavior of $(D_{12})_0(\eta/\eta_0)/W_0$ at high C_2 may be assigned to the corresponding difference in the behavior of μ_{12} shown in Figure 2a.

Salt Stoichiometry on Protein−Salt Interactions

J. Phys. Chem. B, Vol. 110, No. 32, 2006 **16145**

TABLE 3: Thermodynamic Parameters for the Lysozyme−NaCl−H₂O System

C_2 (M)	$(D_{21})_0/(D_{22})_0$	μ_{21}/μ_{22}	$-\Gamma_{\mu_2}$	$\mu_{12}{}^m/RT$ (kg mol⁻¹)	$\mu_{22}{}^m/RT$ (kg mol⁻¹)
0.250	7.02	7.39	4.82	34.3	7.14
0.500	9.87	10.28	5.14	18.7	3.63
0.650	11.53	11.87	5.28	14.9	2.83
0.900	14.24	14.61	5.41	11.3	2.09
1.300	19.06	19.43	6.31	9.5	1.51

TABLE 4: Thermodynamic Parameters for the Lysozyme−MgCl₂−H₂O System

C_2 (M)	$(D_{21})_0/(D_{22})_0$	μ_{21}/μ_{22}	$-\Gamma_{\mu_2}$	$\mu_{12}{}^m/RT$ (kg mol⁻¹)	$\mu_{22}{}^m/RT$ (kg mol⁻¹)
0.0931	3.5	3.8	2.82	76.2	27.0
0.2326	4.6	4.8	2.37	27.8	11.7
0.4642	7.0	7.2	2.49	16.7	6.7
0.9304	12.1	12.3	2.74	12.2	4.5
1.5994	20.2	20.3	4.06	15.3	3.8
1.9995	24.5	24.7	4.39	15.9	3.6

Figure 5. The quotient $(D_{21})_0/(D_{22})_0$ as a function of salt concentration, C_2, for the lysozyme−NaCl−H₂O (○) and the lysozyme−MgCl₂−H₂O (■) systems. Straight lines fit through the data.

Examination of D_{21}. Values of $(D_{21})_V$ for the lysozyme−MgCl₂ and lysozyme−NaCl systems are shown in Figure 1c. The D_{21} values are large and increase with salt concentration. This implies a significant flux of salt due to the concentration gradient of the protein component. One contribution to the value of D_{21} is related to the polyelectrolyte nature of the protein, which is included in the N−H equations. In the presence of a gradient of lysozyme chloride, a flux of both chloride and lysozyme ions is generated. Because $\tilde{D}_{Cl} \gg \tilde{D}_p$, the chloride ions will electrostatically drag the metal ions, yielding a net flux of the salt component and a corresponding positive value of D_{21}. Because the salt component is present in large excess, D_{21} should not depend on C_2 according to N−H equations. Interestingly, contrary to N−H prediction, we observe that D_{21} significantly increases with C_2 well above the constant values predicted by eq 8c. This occurs because a significant contribution to the value of D_{21} can be related to excluded volume effects.[9,19,41] In a solution in which the salt component has a uniform stoichiometric concentration C_2, the presence of protein macromolecules, treated as a second phase, produces an increase in salt concentration in the interstitial volume surrounding them. This interstitial concentration will increase as the protein concentration increases. Therefore, a gradient of C_1 will produce an "effective gradient" of salt in the same direction, leading to a positive contribution to the values of D_{21}.

We further observe that the values of D_{21} for NaCl are higher than those for MgCl₂. This is consistent with the N−H prediction that D_{21} is proportional to $\tilde{D}_M/(z_M\tilde{D}_M + \tilde{D}_{Cl})$. We shall now explain the observed dependence of D_{21} on salt type and concentration by examining the ratio $(D_{21})_0/(D_{22})_0$.

Examination of the Ratio $(D_{21})_0/(D_{22})_0$. According to N−H equations, the ratio D_{21}/D_{22} is equal to $[z_p/(z_M + 1)]/[(\tilde{D}_{Cl} - \tilde{D}_p)/\tilde{D}_{Cl}]$ and independent of $\tilde{D}_M$. Because $[(\tilde{D}_{Cl} - \tilde{D}_p)/\tilde{D}_{Cl}] = 0.935$, we can neglect $\tilde{D}_p$ and approximately write: $D_{21}/D_{22} \approx z_p/(z_M + 1)$, with D_{21}/D_{22} slightly smaller than $z_p/(z_M + 1)$. We also note that, in the limit of $C_2 \to 0$ and $z_pC_1 \ll z_MC_2$, we have: $\mu_{12}/\mu_{22} = \mu_{21}/\mu_{22} = z_p/(z_M + 1)$. This result, together with eq 4c,d, suggests a direct relation between $(D_{21})_0/(D_{22})_0$ and μ_{21}/μ_{22}. From our data in Tables 3 and 4, we indeed observe that

$$\frac{(D_{21})_0}{(D_{22})_0} \approx \frac{\mu_{21}}{\mu_{22}} \tag{12}$$

with $(D_{21})_0/(D_{22})_0$ slightly smaller than μ_{21}/μ_{22}. This implies that
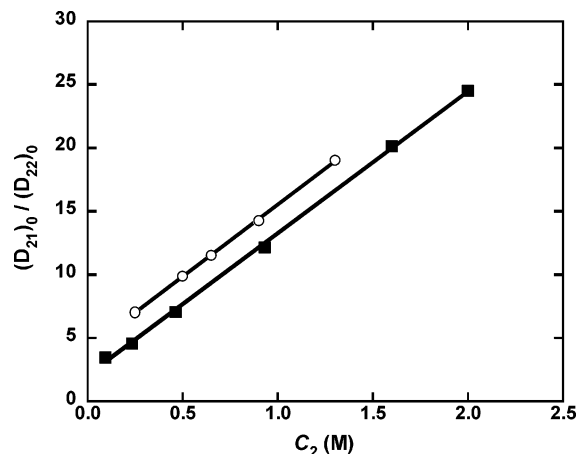
the ratio $(D_{21})_0/(D_{22})_0$ can be used to directly probe the system thermodynamics. Indeed this ratio is essentially a thermodynamic property. This important result is related to the relatively low mobility of proteins. That is, we can approximately describe our system as one in which the lysozyme molecules occupy fixed positions and the fast salt ions partition between high and low protein concentration. When the salt component (and the solvent) reaches equilibrium (μ_2 constant) within this "fixed" gradient of protein, we have $(J_2)_0 = 0$. Then, according to eq 1b, this gives $(D_{21})_0/(D_{22})_0 = -(\partial C_2/\partial C_1)_{\mu_2} = \mu_{21}/\mu_{22}$, consistent with our findings. This argument shows the direct relation of the diffusion method used here to determine thermodynamic quantities and the more traditional equilibrium-dialysis experimental method. In the latter case, the salt partitions (μ_2 constant) between two domains of different protein concentrations separated by a membrane that does not allow the protein to diffuse through. It is important to remark that we do use the rigorous eq 5a,b to determine the ratio μ_{21}/μ_{22}. Yet, the above discussion gives the rationale on why ternary diffusion is valuable in determining protein−salt thermodynamic interactions.

In Figure 5, we report the $(D_{21})_0/(D_{22})_0$ for NaCl and MgCl₂ as a function of C_2. The curves appear to be approximately linear and nearly parallel but with different intercepts (i.e., values at $C_2 = 0$ with $z_pC_1 \ll z_MC_2$). The difference in the intercept between NaCl and MgCl₂ can be assigned to the difference in z_M. Because $(D_{21})_0/(D_{22})_0 \approx z_p/(z_M + 1)$ at $C_2 = 0$, we predict the ratio of the NaCl to the MgCl₂ intercepts to be ≈3/2, assuming that z_p is independent of the type of salt.

To understand the dependence of $(D_{21})_0/(D_{22})_0$ on C_2, we will now consider an excluded-volume model.

The Excluded-Volume Model. This model considers the protein molecules as a second phase not accessible to the small salt ions. This excluded-volume effect produces an increase of small-ion concentration by a factor $1/(1 - C_pV_{ex})$, where C_p is the protein concentration and V_{ex} is the excluded volume per each mole of protein. We assume that the excluded volume is constant and independent of salt concentration, and consider the case of $C_1 \to 0$ so that we can ignore changes in excluded-volume properties due to protein−protein contacts. We also assume that the charge on the protein is constant.

Although the model is a simplification of actual systems, it yields a useful description of our thermodynamic results. According to the excluded volume model, the chemical potential of the salt component becomes

$$(\mu_2 - \mu_2^{\,0})/RT = \ln C_M^{\text{int}} + z_M \ln C_{Cl}^{\text{int}} + (z_M + 1)\ln y_2^{\text{int}} \quad (13)$$

where the interstitial (int) ion concentrations are defined by

$$C_{Cl}^{\text{int}} = \frac{C_{Cl}}{1 - C_p V_{ex}} = \frac{z_p C_1 + z_M C_2}{1 - C_1 V_{ex}} \quad (14a)$$

$$C_M^{\text{int}} = \frac{C_M}{1 - C_p V_{ex}} = \frac{C_2}{1 - C_1 V_{ex}} \quad (14b)$$

and y_2^{int} is the corresponding mean activity coefficient. As in Donnan equilibrium, we assume y_2^{int} to be equal to that of a binary salt solution in equilibrium through a membrane with the ternary mixture. In this case, y_2^{int} will depend only on μ_2. By inserting eq 14a,b into eq 13, we obtain in the limit of $C_1 \to 0$:

$$\frac{\mu_{21}}{\mu_{22}} = -\left(\frac{\partial C_2}{\partial C_1}\right)_{\mu_2} = \frac{z_p}{1 + z_M} + C_2 V_{ex} \quad (15)$$

Accordingly, the change of μ_{21}/μ_{22} and $(D_{21})_0/(D_{22})_0$ is linear with the salt concentration as it has been experimentally found. The intercept is due to the polyelectrolyte nature of the protein and represents the common-ion effect. According to this model, the slope quantifies the excluded volume of the protein. The calculated values of V_{ex} are ∼20% larger than the lysozyme partial molar volumes for both NaCl and MgCl$_2$. These are comparable to the lysozyme hydrodynamic volume.[42]

We will now compare this excluded volume model with a rigorous thermodynamic treatment of the protein−salt interactions.

Protein−Salt Thermodynamic Interactions. Protein−salt thermodynamic interactions are conveniently described by the chemical potential derivatives based on molality, as discussed by Arakawa et al.:[1,25] $\mu_{12}^{(m)} \equiv (\partial\mu_1/\partial\mu_2)_{T,p,m_1} \equiv (\partial\mu_2/\partial\mu_1)_{T,p,m_2}$ and $\mu_{22}^{(m)} \equiv (\partial\mu_2/\partial m_2)_{T,p,m_1}$. These quantities are related to the molarity-based derivatives by

$$\mu_{12}^{(m)} = (d - C_1 M_1 - C_2 M_2)[\mu_{21}(1 - C_1\bar{V}_1) - \mu_{22}C_2\bar{V}_1] \quad (16a)$$

$$\mu_{22}^{(m)} = (d - C_1 M_1 - C_2 M_2)[\mu_{22}(1 - C_2\bar{V}_2) - \mu_{21}C_1\bar{V}_2] \quad (16b)$$

where d is the solution density in g dm^{-3}. The values of $\mu_{12}^{(m)}$ and $\mu_{22}^{(m)}$ obtained using eq 16a,b are reported in Tables 3 and 4, respectively, for NaCl and MgCl$_2$. We observe that the values of $\mu_{12}^{(m)}$ closely match the values of μ_{12}. Another useful parameter reported in Tables 3 and 4 is the preferential interaction coefficient Γ_{μ_2}:[1,25]

$$\Gamma_{\mu_2} \equiv \left(\frac{\partial m_2}{\partial m_1}\right)_{T,\mu_2} = -\frac{\mu_{12}^{(m)}}{\mu_{22}^{(m)}} \quad (17)$$

We now want to consider the relation of the preferential interaction parameters to the excluded volume parameter, V_{ex}. Considering eq 17 and taking the ratio between parts a and b of eq 16 in the limit that $C_1 \to 0$, we obtain:

$$\frac{\mu_{21}}{\mu_{22}} = \Gamma_{\mu_2}(1 - C_2\bar{V}_2) + C_2\bar{V}_1 \quad (18)$$

Because $(1 - C_2\bar{V}_2) \approx 1.0$ for all our measurements (the actual value ranges from 0.96 to 1.00), we neglect this factor
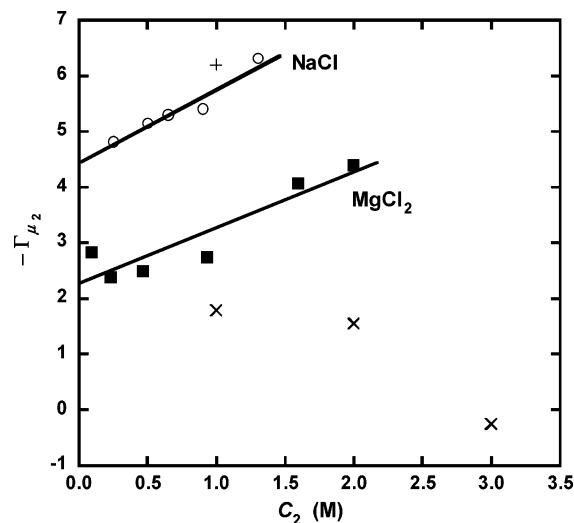
Figure 6. Preferential interaction coefficients reported as $-\Gamma_{\mu_2}$ as a function of salt concentration, C_2, for the lysozyme−NaCl−H$_2$O (○) and the lysozyme−MgCl$_2$−H$_2$O (■) systems. Values at 20 °C taken from ref 39 (NaCl, +), and ref 1 (MgCl$_2$, ×).

and rewrite eq 18 in the following way:

$$-\Gamma_{\mu_2} \approx \frac{z_p}{1 + z_M} + C_2(V_{ex} - V_1) \quad (19)$$

According to eq 19, the preferential interaction parameter is linear in C_2. The intercept represents the common-ion effect as in the case of μ_{21}/μ_{22}. However, the slope is now the difference between the excluded volume and the partial molar volume of the protein. If $\bar{V}_1$ can be assumed to be the volume occupied by the macromolecules, $V_{ex} - \bar{V}_1 > 0$ describes the excess of water surrounding the proteins (preferential hydration), while $V_{ex} - \bar{V}_1 < 0$ describes the excess of salt surrounding the proteins (salt association).[1]

Our results on $-\Gamma_{\mu_2}$ are shown in Figure 6. The values of $-\Gamma_{\mu_2}$ for NaCl are higher than those for MgCl$_2$. By fitting our data with straight lines, we find that the ratio of the two intercepts is 2.0 ± 0.6, consistent with the predicted value of ≈ 3/2. We also find that the two slope values, which are 1.3 ± 0.4 M^{-1} for the NaCl case and 1.0 ± 0.4 M^{-1} for the MgCl$_2$, are positive and approximately equal, as we expected from the parallelism of the two $(D_{21})_0/(D_{22})_0$ plots. This indicates the presence of protein preferential hydration in both cases with a preferential interaction contribution being roughly equal for both systems.

In Figure 6, we include literature values of $-\Gamma_{\mu_2}$ for aqueous lysozyme in NaCl[42] (at $C_2 = 1$ M) and in MgCl$_2$[1] (at $C_2 = 1$, 2, 3 M) in the presence of acetate buffer (HAc/NaAc, 0.05 M, pH 4.5) obtained by equilibrium-dialysis at 20 °C. In the case of NaCl, our $\mu_{12}^{(m)}$ and Γ_{μ_2} are in good agreement with the literature value. In the case of MgCl$_2$, the agreement at $C_2 > 1$ M is not good. Contrary to our results, the slope $V_{ex} - \bar{V}_1$ is negative, suggesting significant Mg^{2+} binding, especially at high salt concentration. Possible sources of discrepancy are the presence of acetate-buffer components in the equilibrium-dialysis experiments and the difference in temperature. However, we are unable to explain the observed differences.

We remark that our results show that the common-ion effect is an important contribution to the protein−salt thermodynamic interaction. It also appears to be the main source of difference between NaCl and MgCl$_2$.

We now consider the behavior of $\mu_{12}^{(m)} \approx \mu_{12}$ as a function of salt type and concentration. This quantity is important because it gives the increase of protein chemical potential as a function of salt concentration. In the case of MgCl$_2$, $\mu_{12}^{(m)} \approx \mu_{12}$ and μ_{21} increase with C_2 at high salt concentration (see Figure 2a,b). This behavior was not observed for NaCl and represents an important difference between the two systems. We note that $\mu_{12}^{(m)} = -\Gamma_{\mu_2} \mu_{22}^{(m)}$. Thus, we can relate the observed differences in $\mu_{12}^{(m)}$ to the thermodynamic properties of the saltwater binary systems,[32,33] represented by $\mu_{22}^{(m)} \approx (z_M + 1)(1 + \partial \ln y_2 / \partial \ln m_2)/m_2$. In agreement with our results, the activity-coefficient term for MgCl$_2$ significantly increases with C_2, but remains relatively small for NaCl.

Summary and Conclusions

In this paper, we have reported the four diffusion coefficients for the lysozyme−MgCl$_2$−water ternary system. The comparison with previous results on the lysozyme−NaCl−water ternary system has allowed us to examine the effect of salt stoichiometry on the transport properties of protein−salt aqueous mixtures. We have found that the cross-diffusion coefficients, D_{12} and D_{21}, are very sensitive to salt stoichiometry. We were able to predict most of the observed differences between the MgCl$_2$ and NaCl cases by taking into account the charges of the metal ions and other properties of binary saltwater mixtures. The salt main-diffusion coefficient, D_{22}, can be directly related to the corresponding binary salt diffusion coefficient. The protein main-diffusion coefficient, D_{11}, is mainly affected by solution viscosity within our experimental domain. However, by reporting $(D_{11})_0(\eta/\eta_0)$ as a function of C_2, we have found the presence of a minimum in the MgCl$_2$ case. This behavior was not observed in the NaCl case. Our results suggest an increase in the thermodynamic factor, μ_{11}, consistent with the presence of protein−protein repulsive interactions at high MgCl$_2$ concentrations, in agreement with literature.

We have used all four ternary diffusion coefficients to extract chemical-potential cross-derivatives (μ_{11} and μ_{21}) and preferential interactions coefficients (Γ_{μ_2}). These thermodynamic data characterize the protein−salt thermodynamic interactions. We have argued that the quotient $(D_{21})_0/(D_{22})_0 \approx \mu_{21}/\mu_{22}$ is essentially a thermodynamic property for both salt cases. This quotient, which linearly increases with salt concentration, can be separated into two parts. The first part, which is independent of salt concentration, can be related to the common-ion effect (or Donnan effect). We have corroborated the presence of common-ion effects by showing that this contribution for the NaCl case is higher than that for the MgCl$_2$ case, consistent with salt stoichiometry. The same result is obtained from our Γ_{μ_2} values. The second part of this quotient, which can be described by an excluded volume model, is directly proportional to salt concentration. The corresponding slope is the volume of the protein molecules including their hydrated shells. We have found that the slope value for the MgCl$_2$ case is about the same as that for the NaCl case, indicating the presence of similar protein preferential hydration for both salt cases. This is confirmed by our Γ_{μ_2} values. We conclude that both common-ion effects and protein preferential hydration are important for describing protein−salt thermodynamic interactions. Our results also indicate that both μ_{11} and μ_{12} are crucial parameters for understanding the complex effect of salt on the protein thermodynamic behavior in solution.

Supporting Information Available: Experimental ternary diffusion results. This material is available free of charge via the Internet at http://pubs.acs.org.

References and Notes

(1) Arakawa, T.; Bhat, R.; Timasheff, S. N. *Biochemistry* **1990**, *29*, 1914.
(2) Timasheff, S. N.; Xie, G. *Biophys. Chem.* **2003**, *105*, 421.
(3) Courtneay, E. S.; Capp, M. W.; Anderson, C. F.; Record, M. T., Jr. *Biochemistry* **2000**, *39*, 4455.
(4) Ducruix, A.; Guilloteau, J.; Riès-Kautt, M.; Tardieu, A. *J. Cryst. Growth* **1996**, *168*, 28.
(5) Curtis, R.; Prausnitz, J. M.; Blanch, H. W. *Biotechnol. Bioeng.* **1998**, *57*, 11.
(6) Minton, A. P. *Curr. Opin. Struct. Biol.* **2000**, *10*, 34.
(7) Annunziata, O.; Asherie, N.; Lomakin, A.; Pande, J.; Ogun O.; Benedek, G. B. *Proc. Natl. Acad. Sci. U.S.A.* **2002**, *99*, 14165.
(8) Retailleau, P.; Ducruix, A.; Riès-Kautt, M. *Acta Crystallogr., Sect. D* **2002**, *58*, 1576.
(9) Annunziata, O.; Paduano, L.; Pearlstein, A. J.; Miller, D. G.; Albright, J. G. *J. Phys. Chem. B* **2006**, *110*, 1405.
(10) McPherson, A. *Crystallization of Biological Macromolecules*; Cold Spring Harbor Laboratory Press: Plainview, N, 1998.
(11) Rosenberger, F.; Vekilov, P. G.; Muschol, M.; Thomas, B. R. *J. Cryst. Growth* **1996**, *167*, 1.
(12) Tardieu, A.; Bonnete, F.; Finet, S.; Vivares, D *Acta Crystallogr., Sect. D* **2002**, *58*, 1549.
(13) Liu, W.; Cellmer, T.; Keerl, D.; Prausnitz, J. M.; Blanch, H. W. *Biotechnol. Bioeng.* **2005**, *90*, 482.
(14) Ru, M. T.; Hirokane, S. Y.; Lo, A. S.; Dordick, J. S.; Reimer, J. A.; Clark, D. S. *J. Am. Chem. Soc.* **2000**, *122*, 1565.
(15) Wyman, J., Jr. *Adv. Protein Chem.* **1964**, *19*, 223.
(16) Clark, E. D. *Curr. Opin. Biotechnol.* **2001**, *12*, 202.
(17) George, A.; Wilson, W. W. *Acta Crystallogr., Sect. D* **1994**, *50*, 361.
(18) Finet, S.; Skouri-Panet, F.; Casselyn, M.; Bonnete, F.; Tardieu, A. *Curr. Opin. Colloid Interface Sci.* **2004**, *9*, 112.
(19) Annunziata, O.; Paduano, L.; Pearlstein, A. J.; Miller, D. G.; Albright, J. G. *J. Am. Chem. Soc.* **2000**, *122*, 5916.
(20) Leaist, D. G. *J. Phys. Chem.* **1989**, *93*, 474.
(21) Albright, J. G.; Annunziata, O.; Miller, D. G.; Paduano, L.; Pearlstein A. J. *J. Am. Chem. Soc.* **1999**, *121*, 3256.
(22) Paduano, L.; Annunziata, O.; Pearlstein, A. J.; Miller, D. G.; Albright, J. G. *J. Cryst. Growth* **2001**, *232*, 273.
(23) Tanford, C. *Physical Chemistry of Macromolecules*; Wiley: New York, 1961.
(24) Warren, P. B. *J. Phys.: Condens. Matter* **2002**, *14*, 7617.
(25) We use the subscript "1" for the protein component and the subscript "2" for the salt component, consistent with the literature on multicomponent diffusion. However, the subscript "2" for the protein component and the subscript "3" for the salt component are extensively used in relation to the thermodynamic description of protein mixtures.
(26) Gosting, L. J. *Adv. Protein Chem.* **1956**, *11*, 429.
(27) Kirkwood, J. G.; Baldwin, R. L.; Dunlop, P. J.; Gosting, L. J.; Kegeles, G. *J. Chem. Phys.* **1960**, *33*, 1505.
(28) Dunlop, P. J.; Gosting, L. J. *J. Phys. Chem.* **1959**, *63*, 86.
(29) Woolf, L. A.; Miller, D. G.; Gosting, L. J. *J. Am. Chem. Soc.* **1962**, *84*, 317.
(30) Miller, D. G. *J. Phys. Chem.* **1986**, *90*, 1509.
(31) Miller, D. G. *J. Phys. Chem.* **1959**, *63*, 570.
(32) Miller, D. G.; Rard, A. J.; Eppstein, L. B.; Albright, J. G. *J. Phys. Chem.* **1984**, *88*, 5739.
(33) Rard, J. A.; Miller, D. G. *J. Sol. Chem.* **1979**, *8*, 701.
(34) Tanford, C.; Wagner, M. L. *J. Am. Chem. Soc.* **1954**, *76*, 3331.
(35) Annunziata, O.; Buzatu, D.; Albright, J. G. *Langmuir* **2005**, *21*, 12085.
(36) Robinson, R. A.; Stokes, R. H. *Electrolyte Solutions*; Academic Press: New York, 1955.
(37) Isono, T. *J. Chem. Eng. Data* **1984**, *29*, 45.
(38) Zhang, H.-L.; Han, S.-J. *J. Chem. Eng. Data* **1996**, *41*, 516.
(39) Grisby, J. J.; Blanch, H. W.; Prausnitz, J. M. *J. Phys. Chem. B* **2000**, *104*, 3645.
(40) Miller, D. G. *J. Phys. Chem.* **1967**, *71*, 616.
(41) Vergara, A.; Paduano, L.; Vitagliano V.; Sartorio R. *Mater. Chem. Phys.* **2000**, *66*, 126.
(42) Arakawa, T.; Timasheff, S. N. *Biochemistry* **1984**, *23*, 5912.